VIP Azopolymers Very Important Paper

International Edition: DOI: 10.1002/anie.201510796
German Edition: DOI: 10.1002/ange.201510796

Tuning and Erasing Surface Wrinkles by Reversible Visible-Light-Induced Photoisomerization

Chuanyong Zong[+], Yan Zhao[+], Haipeng Ji, Xue Han, Jixun Xie, Juanjuan Wang, Yanping Cao, Shichun Jiang,* and Conghua Lu**

Abstract: *Periodic wrinkling across different scales has received considerable attention because it not only represents structure failure but also finds wide applications. How to prevent wrinkling or create desired wrinkling patterns is non-trivial because the dynamic evolution of wrinkles is a highly nonlinear problem. Herein, we report a simple yet powerful method to dynamically tune and/or erase wrinkling patterns with visible light. The light-induced photoisomerization of azobenzene units in azopolymer films leads to stress release and consequently to the erasure of the wrinkles. The wrinkles in unexposed regions are also affected and oriented perpendicular to the exposed boundary during the stress reorganization. Theoretical models were developed to understand the dynamics of the reversible photoisomerization-induced wrinkle evolution. This method can be applied for designing functional materials/devices, for example, for the reversible optical writing/erasure of information as demonstrated here.*

Surface wrinkling of a soft material with a hard skin is ubiquitous in both nature and engineering.[1,2] Compressive stress is often incurred in the hard skin because of an inhomogeneous or anisotropic distribution of deformation that arises from structural heterogeneities, non-uniform microenvironments, and/or spatial limitations in available nutrients.[1,2] Once the compressive stress, σ, in the skin exceeds the critical stress, σ_c, surface wrinkling may occur to minimize the total potential energy of the system. Surface wrinkling may pose a limit on the performance of structures and is often thought to be a nuisance.[3] On the other hand, owing to their characteristics, wrinkles have found broad applications ranging from characterizing the mechanical properties of ultrathin films[4] and creating tunable patterns[5] and functional surfaces[6–8] to designing flexible electronics and advanced photovoltaics.[9,10]

Emulating and leveraging surface wrinkling requires an understanding of both σ_c, which depends on the physical and geometrical parameters of the system, and σ, which depends on various external or internal stimuli. For a given system, a number of theoretical and computational models have been proposed that enable us to predict σ_c.[11,12] However, reliable manipulation of stress states in the system to control wrinkling patterns remains a challenging issue and has received considerable interest in the past few years. Aside from controlling the magnitude of the external/internal stimuli,[13] a desired stress/deformation state may be achieved by modifying the topographic features on the underlying substrates[1,14] or stiff films,[15,16] by making use of curvature effects,[17] and/or by adopting template-directed confinement effects.[18]

Herein, we report a simple yet powerful method to dynamically tune and/or erase the surface wrinkles on an azo-containing poly(disperse orange 3) (PDO_3) film bonded to a poly(dimethylsiloxane) (PDMS) substrate with visible light. Upon light irradiation, reversible photoisomerization of the azobenzene moieties in the wrinkled PDO_3 film takes place, leading to the release of the internal stress. Our experiments in combination with our theoretical model reveal that the continuous variation of the stress field decreases the wrinkle amplitude and finally erases the wrinkling patterns in the exposed region. The wrinkles around the unexposed region are dynamically tuned during the selective exposure and oriented towards the exposed boundary owing to the boundary effect.[1,19] We demonstrate that this optically controlled wrinkling system can be used for the reversible optical writing and erasure of (classified) information. Furthermore, the current strategy may be applied for eliminating undesired surface wrinkles and fabricating functional surfaces with tunable friction, adhesion, wetting, and optical properties.

The key steps to tune and/or erase surface wrinkles in the PDO_3/PDMS system with visible light are illustrated in Figure 1. The PDO_3-based film/substrate system is fabricated

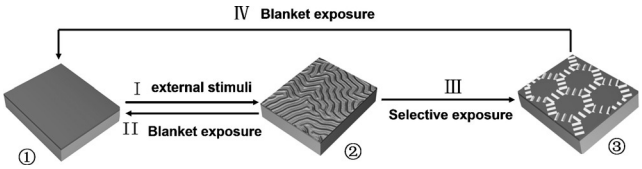

Figure 1. Schematic illustration of the procedure to optically tune and erase the surface wrinkles on a PDO_3/PDMS bilayer with visible light. I) Surface wrinkling is induced by external stimuli. II) Optical erasure of the wrinkles by blanket exposure. III) Prescribed erasure of the wrinkles by selective exposure through copper grids or photomasks. IV) Blanket exposure of a previously selectively exposed bilayer to fully erase the wrinkles.

[*] C. Zong,[+] H. Ji, X. Han, J. Xie, J. Wang, Prof. S. Jiang, Prof. C. Lu
School of Materials Science and Engineering
Tianjin University, Tianjin, 300072 (China)
E-mail: scjiang@tju.edu.cn
chlu@tju.edu.cn
Y. Zhao,[+] Prof. Y. Cao
AML, Department of Engineering Mechanics
Tsinghua University, Beijing, 100084 (China)
E-mail: caoyanping@tsinghua.edu.cn
[+] These authors contributed equally to this work.

Supporting information for this article can be found under http://dx.doi.org/10.1002/anie.201510796.

 © 2016 Wiley-VCH Verlag GmbH & Co. KGaA, Weinheim

by spin-coating a PDO_3 layer onto the PDMS substrate (① in Figure 1). With the help of external stimuli, surface wrinkling, typically with sinusoidal profiles, is induced in the film/substrate bilayer once the critical wrinkling conditions are met (i.e., ①→②, step I in Figure 1). In the case of blanket exposure of the wrinkled bilayer to visible light, the wrinkles are erased, and a smooth surface is obtained (i.e., ②→①, step II). Upon selective exposure through copper grids or photomasks, the surface wrinkles in the exposed region are erased and those in the unexposed part are kept with the wrinkles oriented perpendicular to the exposed/unexposed boundary (i.e., ②→③, step III). The resulting patterned wrinkles can be thoroughly erased by subsequent blanket exposure, which transforms the whole surface into a wrinkle-free state (i.e., ③→①, step IV). The above wrinkling/de-wrinkling cycle is repeatable (for details see the Supporting Information).

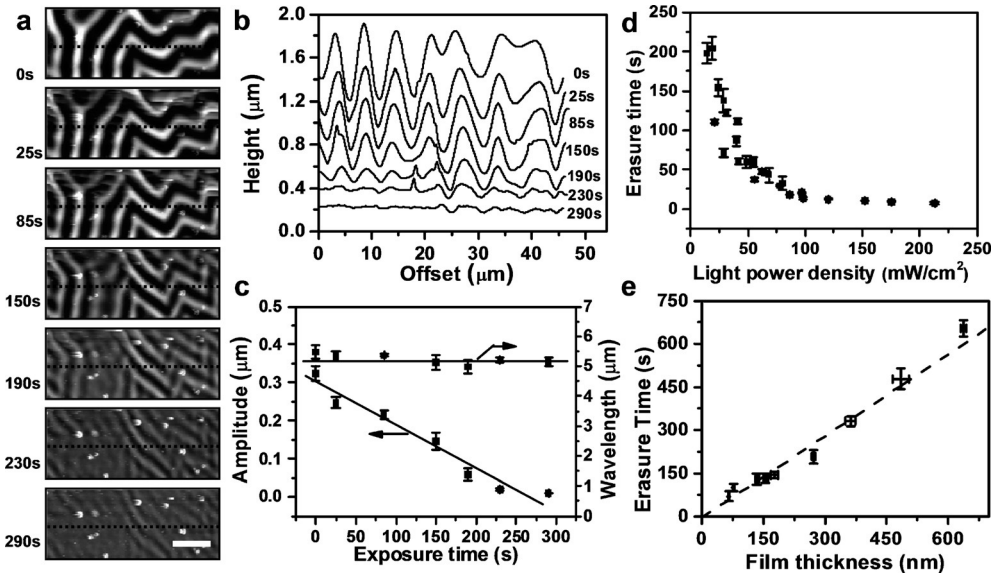

Figure 2. a–c) Wrinkle evolution during the blanket exposure of the wrinkled bilayer. a) AFM height images, b) AFM cross-sections, and c) dependence of the wrinkle amplitude A and wavelength λ on the exposure time t. d, e) Dependence of the optical erasure time t_e on the light power density I_{opd} ($h_f = 300$ nm) and the film thickness h_f ($I_{opd} = 18.5$ mW cm^{-2}), respectively. Scale bar: 10 μm.

The maximum peak in the UV/Vis absorption spectrum of PDO_3 (Supporting Information, Figure S1 a), which was synthesized by solid polymerization,[20] is observed at approximately 478 nm (Figure S1 b). Owing to the mismatch in the thermal expansion coefficients of the elastic PDMS substrate and the stiff PDO_3 film, an equibiaxial compressive stress σ is generated upon cooling a bilayer that had been heated to 90 °C. Once $\sigma > \sigma_c$, the formation of surface wrinkles is induced (Figure S1 c, d). Here, σ_c is determined by the bilayer properties with $\sigma_c = \frac{1}{4}\bar{E}_f\left(3\bar{E}_s/\bar{E}_f\right)^{2/3}$, where the plane strain modulus is given by $\bar{E} = E/\left(1-\nu^2\right)$; E is the Young's modulus, and ν is the Poisson's ratio. The subscripts f and s refer to the film and the substrate, respectively. The critical wrinkling wavelength (λ) is determined by:[12,21]

$$\lambda = 2\pi h_f \left(\frac{\bar{E}_f}{3\bar{E}_s}\right)^{1/3} \quad (1)$$

The wrinkle amplitude (A) depends on the film thickness (h_f), the critical wrinkling strain (ε_c), and the pre-strain (ε_{pre}) according to:[21]

$$A \propto h_f \sqrt{\frac{\varepsilon_{pre}}{\varepsilon_c} - 1} \quad (2)$$

Equations (1) and (2) show that both λ and A of the resulting wrinkles linearly depend on h_f (Figure S1 e).

Interestingly, the above wrinkle morphologies can be maintained in the dark for long periods of time (e.g., six months). In contrast, exposure to visible light leads to the gradual erasure of the labyrinth wrinkles (Figure 2; see also Figure S2), irrespective of the light polarization (Figure S3). However, the optical erasure is dependent on the light wavelength applied ($\lambda \approx 410$–550 nm; see Table S1), which has to correspond to the absorption band of the PDO_3 film (Figure S1 b). Herein, we also carefully examined the evolution of the wrinkle morphologies with light irradiation. According to the results of the in situ AFM characterization, the wrinkle wavelength λ does not change significantly while the wrinkle amplitude A decreases linearly with the exposure time (t; Figure 2 b, c). Furthermore, the optical erasure time (t_e), which is the time required to completely erase the wrinkles, is strongly dependent on the light power density, I_{opd}, h_f, and A (Figure 2 d, e; see also Figure S4). As shown in Figure 2 d, for a given h_f, t_e scales with I_{opd}. For example, for $h_f = 300$ nm, $t_e \approx I_{opd}^{-1.27}$. When I_{opd} is kept constant, t_e is basically linear to h_f (Figure 2 e). The t_e value is also related to A owing to the dependence of A on h_f and the pre-strain ε_{pre} as shown in Eq. (2) and Figure S4, as well as the correlation between A and t (Figure 2 c).

When the whole wrinkled PDO_3/PDMS bilayer is exposed to light, the wrinkles are globally erased. We further investigated the selective exposure of the wrinkled bilayer through copper grids with different exposed/unexposed regions. For simplicity, the exposed part is denoted as D_1, and the unexposed part is denoted as D_2 (Figure S5). The labyrinth wrinkles in the exposed region D_1 have been fully erased after light irradiation (Figure 3; see also Figures S6–S8). In situ optical analysis (Movie S1 and Figure S6) clearly shows that the erasure process of the wrinkles in D_1 is similar to that

 © 2016 Wiley-VCH Verlag GmbH & Co. KGaA, Weinheim

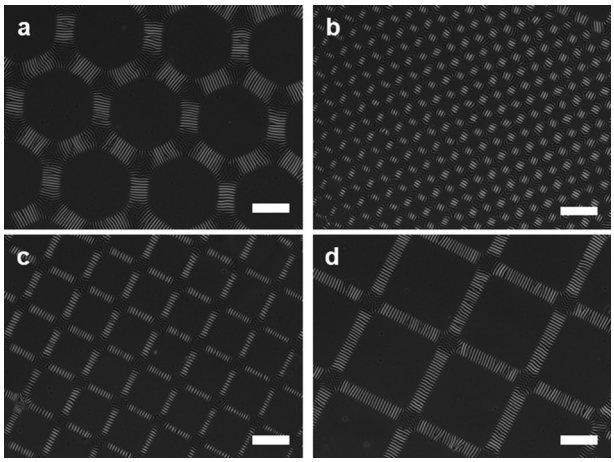

Figure 3. Optical images of the hierarchical patterns obtained when the wrinkled PDO_3/PDMS bilayer was selectively exposed to light through the copper grids H50 (a), R400 (b), S300 (c), and S200 (d). Scale bars: 100 μm.

observed upon blanket exposure in Figure 2. Surprisingly, the initially disordered wrinkles in the unexposed region D_2 have dynamically evolved into highly ordered wrinkles with almost unchanged wrinkle wavelengths during the irradiation (Movie S2 and Figure S6). In the final states, these wrinkles are oriented perpendicular to the D_1/D_2 boundary, irrespective of the wrinkle wavelength of the initial labyrinth patterns (Figure S7) and the geometries and sizes of the boundary (the copper grids; Figure 3 and Figure S8). This orientation change in D_2 is due to the boundary effect and the consequence of the dynamic evolution of the stress field that is induced by the photoisomerization of the azopolymer film (see below).

Azobenzene chromophores are known to have a stable *trans* state and a metastable *cis* state.[22] These two isomeric states have different dipole moments and molecular lengths (0.5 D/0.9 nm and 3.1 D/0.55 nm for the *trans* and *cis* states, respectively, for azobenzene itself).[23] Similar to other pseudo-stilbene azo molecules,[24] the *trans* and *cis* absorption bands of the azo-containing PDO_3 overlap (Figure S1 a, b). When the PDO_3 film is irradiated with light of the correct wavelength (Table S1), the *trans* and *cis* states are simultaneously transferred to an electronically excited state, and the azobenzene chromophore undergoes reversible *trans*/*cis* photoisomerization.[24] Furthermore, the azobenzene chromophore of PDO_3 has a higher polarizability than the main-chain azopolymer because of the substituted acceptor and thus a shorter excited-state lifetime.[24,25] As the *trans*/*cis* states have different structures, the rapid reversible *trans*/*cis* cycles will generate a significant nanoscale force[26] and require an increase in spatial volume[23] for the local movement/transition of the azobenzene chromophores in the side chain and the motion of the polymer backbone. Consequently, the reversible *trans*/*cis* cycling has the following effects on the exposed PDO_3 film.

First of all, a photosoftening effect is observed, which has also been experimentally identified in several other azo-containing systems.[27] In our study, the nanoindentation results show that the decrease in the Young's modulus of the PDO_3 film that is caused by the light irradiation is about 58–72 % (Figure S9). Owing to the expansion effect that is induced by the creation of extra free volume for the *trans*/*cis* photoisomerization, the film thickness increases by approximately 4 % according to the AFM characterization (Figure S10), which is generally consistent with previous reports on other azo-containing films.[28]

Aside from the above photosoftening effect, the rapid reversible *trans*/*cis* photoisomerization will generate a localized force[23,26] and induce the continuous disturbance of the localized stress field in the wrinkled film. As a result, the residual stress in the wrinkled system is released, and the stress field is modulated, resulting in the spontaneous adjustment of the wrinkle morphologies. In our case, the wrinkle amplitude gradually decreases with the stress release in the exposed region. When the critical wrinkling conditions are not satisfied anymore, the wrinkles are fully erased.

To identify the role of the photosoftening effect and the stress release induced by the reversible photoisomerization of azobenzene, computational studies based on the spectral[29] and the finite-element method were performed. In the simulations based on the spectral method, the film was modeled as the von Karman plate, and the substrate was assumed to be a linear elastic half space. Fast Fourier transform analysis was used to calculate the spatial differentiations in the plate equations. Periodic boundary conditions were imposed. Prior to selective exposure, the membrane strains in the film are given by[29]

$$\varepsilon_{\alpha\beta} = \varepsilon^0_{\alpha\beta} + \left(u_{\alpha,\beta} + u_{\beta,\alpha}\right)/2 + w_{,\alpha} w_{,\beta}/2 \tag{3}$$

where $\varepsilon^0_{\alpha\beta}$ is the initial strain, u_α refers to the in-plane displacement field, and w is the normal deflection. The Greek subscripts in all equations take the values 1 and 2, and repeated Greek subscripts represent summation from 1 to 2. The membrane forces related to the membrane strains are

$$N_{\alpha\beta} = h_f \bar{E}_f \left[(1-\nu_f)\varepsilon_{\alpha\beta} + \nu_f \varepsilon_{\gamma\gamma}\delta_{\alpha\beta}\right] \tag{4}$$

where $\delta_{\alpha\beta}$ is the Kronecker delta. The in-plane and out-of-plane equilibrium equations are given by

$$N_{\alpha\beta,\beta} = T_\alpha \tag{5}$$

$$T_3 = -\frac{1}{12}\bar{E}_f h_f^3 w_{,\alpha\alpha\beta\beta} + \left(N_{\alpha\beta} w_{,\alpha}\right)_{,\beta} \tag{6}$$

where T_1 and T_2 are the interfacial shear tractions between the film and the substrate, and T_3 is the normal traction. T_α and T_3 can be obtained by solving the elastic field of the substrate.[29] When the PDO_3/PDMS system was exposed to light, the membrane strains/stresses in the film are gradually released owing to the reversible photoisomerization of azobenzene. The membrane strains are modified according to

$$\varepsilon^*_{\alpha\beta} = \varepsilon_{\alpha\beta} + \xi \tag{7}$$

where ξ refers to the strain relief induced by the reversible photoisomerization and is dependent on the irradiation time t and the applied I_{opd} (Figure 2 d).

 © 2016 Wiley-VCH Verlag GmbH & Co. KGaA, Weinheim

In the case of blanket exposure, the wrinkle amplitude is supposed to be reduced when the membrane strain is gradually released. Eq. (2) well explains this amplitude-reducing process observed upon blanket exposure (Figure 2). When the compressive strain becomes lower than the critical strain, the wrinkles can be fully erased. A simulation result was obtained for a representative example, namely for selective exposure with one composite copper grid with four kinds of meshes (Figure 4; see also Movie S2 and Figure S5e). In the simulations, a film thickness of 0.274 μm was assumed. The modulus ratio, E_f/E_s, was 755, and the Poisson's ratios were both taken to be 0.5. The wrinkling wavelength was 10.9 μm, which is in the range of the values observed in the experiments. Prior to selective exposure, the system exhibited disordered labyrinth patterns (Figure 4I, a). When the system was subjected to selective exposure, the membrane strain was reduced, and the wrinkle amplitude in the exposed region decreased gradually, until the wrinkles were fully erased (Figure 4I, b–g; see also Movie S3). The initially disordered wrinkles in the unexposed region became highly ordered and were oriented perpendicularly to the boundary of the exposed region (Figure 4I, f) because of the boundary effect.[1,19,30] The evolution of wrinkling patterns for different masks, which led to similar phenomena, is shown in Movies S4–S6. To investigate the role of the reduced film modulus in erasing the wrinkles, finite-element simulations were performed (Figure 4II). Sinusoidal wrinkling patterns were observed when a uniform film was subjected to uniaxial compression (Figure 4II, h). When the modulus of the central region of the film is decreased, the wrinkling pattern will evolve to lower the total potential energy of the system. The strain in the surrounding stiff region is released, and the compression in the soft middle region increases. De-wrinkling occurs first in the stiff region, while the wavelength in the soft region becomes smaller (Figure 4II, i–m). This wrinkle evolution induced by the modulus reduction (Figure 4II) is not in accord with our experimental phenomena, indicating that the photosoftening does not play a dominant role here although it corresponds to a greater critical wrinkling strain. Instead, photoisomerization-induced stress/strain release is the key to erasing the wrinkles. In a recent study,[31] Takeshima et al. observed a decrease in the wrinkle wavelength during UV irradiation of a system consisting of azobenzene-containing liquid crystalline polymers that was due to photosoftening.[31] In our system, the surface wrinkles are erased by photoisomerization-induced stress release/reorganization. In this sense, the underlying physical concepts are entirely different from those reported by Takeshima et al. Moreover, our theoretical analysis has clearly shown that photoisomerization-induced stress release is much more powerful than the photosoftening mechanism in either erasing or generating desired surface wrinkles.

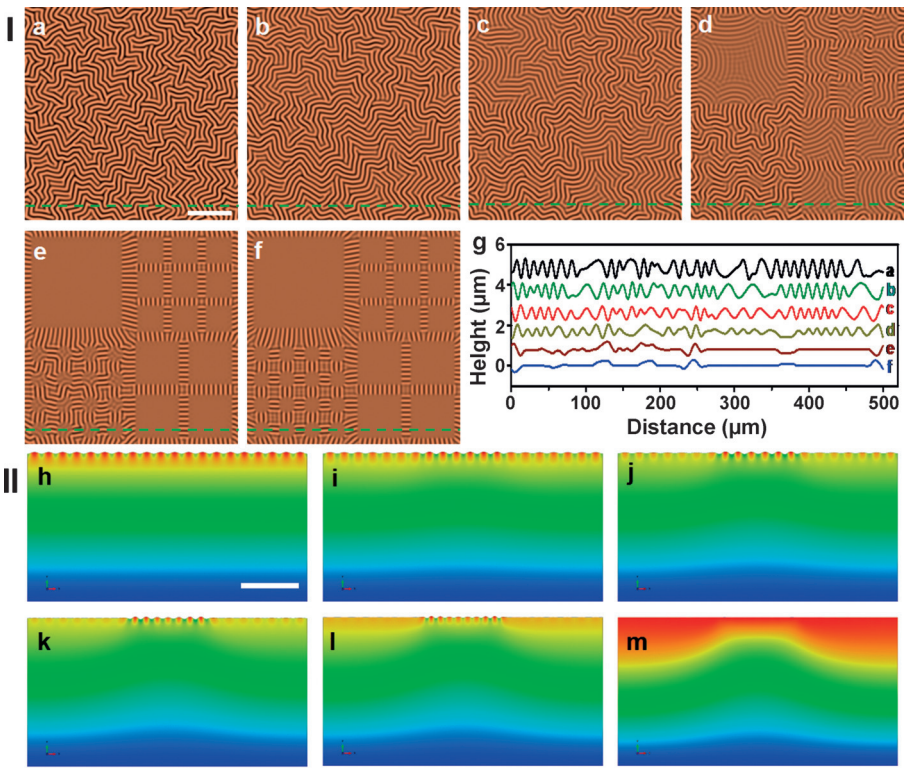

Figure 4. Theoretical simulations of the pattern evolution of the wrinkled system during selective exposure. I) Height images (a–f) and cross-sections (g) of a typical example under selective exposure simulated by the spectral method. a–f) The exposed region was initially subjected to biaxial compression with a compressive strain of 1% (a), 0.8% (b), 0.6% (c), 0.4% (d), 0.2% (e), and 0% (f). II) Wrinkling pattern evolution of a planar strain system simulated by the finite-element method. h) The initially uniform film was subjected to uniaxial compression of 1%. The modulus of the middle region of the film was reduced by 18% (i), 36% (j), 54% (k), 72% (l), and 90% (m). Scale bars: 100 μm (I), 50 μm (II).

By means of the simple selective exposure, we obtained highly ordered wrinkle patterns with well-defined microstructures (Figure 3). As this system does not pose special limitations, large-area selective wrinkle erasure can be very conveniently realized (Figure 5). The resulting exposed/unexposed regions can be easily identified because the unexposed part has a lower transmittance and stronger scattering owing to the presence of wrinkles (Figure 5c,d). Furthermore, as expected, the wrinkles in the unexposed part can be thoroughly erased by blanket exposure, which leads to the formation of a globally wrinkle-free surface. Here, the first, selective exposure can be regarded as the process of "writing" information, and the second, blanket exposure represents the step of erasing the information. Thus, taking advantage of the optical erasability of the current wrinkles combined with the reversible stimulus-induced wrinkling/selective exposure/blanket exposure procedure, we can repeatedly optically write and erase information (Figures 1 and 5). The storage density can be easily tuned by

 © 2016 Wiley-VCH Verlag GmbH & Co. KGaA, Weinheim

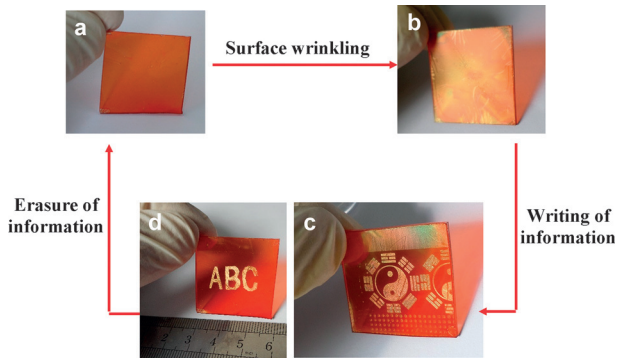

Figure 5. Application of the optically erasable wrinkling system for the repetitive optical writing/erasure of information by multiple cycles of stimulus-induced wrinkling, selective exposure, and blanket exposure.

the mask dimensions (Figures 3 and 5c), and the writing/erasure velocity is determined by the light power density (Figure 2d) and the film thickness (Figure 2e).

In conclusion, we have demonstrated a simple method to tune or erase surface wrinkles on an amorphous azo-based PDO_3 film by modulating the local stress field by visible-light irradiation. A theoretical model has been built to reveal the physics behind the experimental observations. Our analysis indicates that the stress/strain release that is due to the reversible photoisomerization of the azobenzene units in the film plays a key role. The wrinkles can be erased when the whole system is exposed to light. However, selective exposure enables the fabrication of highly ordered wrinkle patterns with well-defined hierarchical microstructures over large areas. The characteristics of our light-responsive composite system can enable unprecedented applications, such as the repetitive optical writing/erasure of (classified) information, eliminating undesired surface wrinkles, and the large-scale fabrication of functional surfaces with desired friction, adhesion, wetting, and optical properties. Owing to the unique advantages of light stimuli (e.g., neatness, non-contact operation, and suitability for remote operation), our method is applicable to surfaces with arbitrary profiles and can also be applied when other methods to modulate the stress state fail. We envision that our light-induced stress-release mechanism can be extended to other functional film/substrate systems for the optical control of surface patterns.

Acknowledgements

C.H.L. acknowledges financial support from the Natural Science Foundation of China (21574099, 21374076). Y.P.C. acknowledges financial support from the NSFC (11172155, 11572179).

Keywords: azopolymers · isomerization · mechanical properties · photochemistry · wrinkling

How to cite: *Angew. Chem. Int. Ed.* **2016**, *55*, 3931–3935
Angew. Chem. **2016**, *128*, 3999–4003

[1] N. Bowden, S. Brittain, A. G. Evans, J. W. Hutchinson, G. M. Whitesides, *Nature* **1998**, *393*, 146–149.
[2] B. Li, Y.-P. Cao, X.-Q. Feng, H. Gao, *Soft Matter* **2012**, *8*, 5728–5745.
[3] A. Carlson, A. M. Bowen, Y. Huang, R. G. Nuzzo, J. A. Rogers, *Adv. Mater.* **2012**, *24*, 5284–5318.
[4] C. M. Stafford, C. Harrison, K. L. Beers, A. Karim, E. J. Amis, M. R. VanLandingham, H.-C. Kim, W. Volksen, R. D. Miller, E. E. Simonyi, *Nat. Mater.* **2004**, *3*, 545–550.
[5] J. Rodríguez-Hernández, *Prog. Polym. Sci.* **2015**, *42*, 1–41.
[6] E. P. Chan, A. J. Crosby, *Adv. Mater.* **2006**, *18*, 3238–3242.
[7] H. J. Bae, S. Bae, C. Park, S. Han, J. Kim, L. N. Kim, K. Kim, S. H. Song, W. Park, S. Kwon, *Adv. Mater.* **2015**, *27*, 2083–2089.
[8] L. B. Lv, T. L. Cui, B. Zhang, H. H. Wang, X. H. Li, J. S. Chen, *Angew. Chem. Int. Ed.* **2015**, *54*, 15165–15169; *Angew. Chem.* **2015**, *127*, 15380–15384.
[9] J. A. Rogers, T. Someya, Y. Huang, *Science* **2010**, *327*, 1603–1607.
[10] J. B. Kim, P. Kim, N. C. Pégard, S. J. Oh, C. R. Kagan, J. W. Fleischer, H. A. Stone, Y.-L. Loo, *Nat. Photonics* **2012**, *6*, 327–332.
[11] H. Allen, *Analysis and design of structural sandwich panels*, Pergamon, Oxford, **1969**.
[12] X. Chen, J. W. Hutchinson, *J. Appl. Mech.* **2004**, *71*, 597–603.
[13] Q. Wang, L. Zhang, X. Zhao, *Phys. Rev. Lett.* **2011**, *106*, 118301.
[14] J. Yoon, P. Bian, J. Kim, T. J. McCarthy, R. C. Hayward, *Angew. Chem.* **2012**, *124*, 7258–7261.
[15] J. Kim, J. A. Hanna, M. Byun, C. D. Santangelo, R. C. Hayward, *Science* **2012**, *335*, 1201–1205.
[16] M. D. Huntington, C. J. Engel, T. W. Odom, *Angew. Chem.* **2014**, *126*, 8255–8259.
[17] N. Stoop, R. Lagrange, D. Terwagne, P. M. Reis, J. Dunkel, *Nat. Mater.* **2015**, *14*, 337–342.
[18] P. J. Yoo, K. Y. Suh, S. Y. Park, H. H. Lee, *Adv. Mater.* **2002**, *14*, 1383–1387.
[19] J.-W. Wang, B. Li, Y.-P. Cao, X.-Q. Feng, *J. Appl. Mech.* **2015**, *82*, 051009.
[20] S. Lee, J. Shin, H. S. Kang, Y. H. Lee, J. K. Park, *Adv. Mater.* **2011**, *23*, 3244–3250.
[21] S. Cai, D. Breid, A. J. Crosby, Z. Suo, J. W. Hutchinson, *J. Mech. Phys. Solids* **2011**, *59*, 1094–1114.
[22] G. Hartley, *Nature* **1937**, *140*, 281.
[23] G. S. Kumar, D. Neckers, *Chem. Rev.* **1989**, *89*, 1915–1925.
[24] H. D. Bandara, S. C. Burdette, *Chem. Soc. Rev.* **2012**, *41*, 1809–1825.
[25] N. Viswanathan, D. Kim, S. Tripathy, *J. Mater. Chem.* **1999**, *9*, 1941–1955.
[26] T. Hugel, N. B. Holland, A. Cattani, L. Moroder, M. Seitz, H. E. Gaub, *Science* **2002**, *296*, 1103–1106.
[27] Y. Zhao, T. Ikeda, *Smart light-responsive materials: azobenzene-containing polymers and liquid crystals*, Wiley, Hoboken, **2009**.
[28] O. M. Tanchak, C. J. Barrett, *Macromolecules* **2005**, *38*, 10566–10570.
[29] Z. Huang, W. Hong, Z. Suo, *J. Mech. Phys. Solids* **2005**, *53*, 2101–2118.
[30] W. Ding, Y. Yang, Y. Zhao, S. Jiang, Y. Cao, C. Lu, *Soft Matter* **2013**, *9*, 3720–3726.
[31] T. Takeshima, W.-y. Liao, Y. Nagashima, K. Beppu, M. Hara, S. Nagano, T. Seki, *Macromolecules* **2015**, *48*, 6378–6384.

Received: November 26, 2015
Revised: January 22, 2016
Published online: February 19, 2016

 © 2016 Wiley-VCH Verlag GmbH & Co. KGaA, Weinheim